Cubic-quintic solitons in the checkerboard potential

Rodislav Driben,[1] Boris A. Malomed,[2] Arthur Gubeskys,[2] and Joseph Zyss[1]
[1]*Laboratoire de Photonique Quantique et Moléculaire, CNRS, École Normale Supérieure de Cachan, UMR 8537, 94235 Cachan, France*
[2]*Department of Physical Electronics, School of Electrical Engineering, Faculty of Engineering, Tel Aviv University, Tel Aviv 69978, Israel*

(Received 15 September 2007; published 7 December 2007)

We introduce a two-dimensional (2D) model which combines a checkerboard potential, alias the Kronig-Penney (KP) lattice, with the self-focusing cubic and self-defocusing quintic nonlinear terms. The beam-splitting mechanism and soliton multistability are explored in this setting, following the recently considered 1D version of the model. Families of single- and multi-peak solitons (in particular, five- and nine-peak species naturally emerge in the 2D setting) are found in the semi-infinite gap, with both branches of bistable families being robust against perturbations. For single-peak solitons, the variational approximation (VA) is developed, providing for a qualitatively correct description of the transition from monostability to the bistability. 2D solitons found in finite band gaps are unstable. Also constructed are two different species of stable vortex solitons, arranged as four-peak patterns ("oblique" and "straight" ones). Unlike them, compact "crater-shaped" vortices are unstable, transforming themselves into randomly walking fundamental beams.

DOI: 10.1103/PhysRevE.76.066604 PACS number(s): 05.45.Yv, 42.65.Tg, 42.70.Nq, 03.75.Lm

I. INTRODUCTION AND THE MODEL

A subject which has drawn much attention in nonlinear optics is the dynamics of spatial solitons (self-trapped beams) in multichannel systems. The multichannel structure is defined through an effective periodic transverse potential, which can be induced by periodic spatial modulation of the local refractive index. More sophisticated structures may be built in photonic crystals. A paradigmatic model which describes the multichannel system in the usual paraxial approximation (assuming that the transverse size of the channels is essentially larger than the carrier wavelength) is based on the generalized nonlinear Schrödinger (NLS) equation for local amplitude $u(z,x,y)$ of the electromagnetic wave propagating along the z axis in a bulk waveguide with the refractive index, $n_0(x,y)$, subject to the periodic modulation in the transverse plane (x,y). In the normalized form, the NLS equation is

$$i\frac{\partial u}{\partial z}+\left(\frac{\partial^2}{\partial x^2}+\frac{\partial^2}{\partial y^2}\right)u+n_0(x,y)u+\delta n(|u|^2)u=0, \qquad (1)$$

with $\delta n(|u|^2)$ a nonlinear correction to the refractive index; in the case of the ordinary Kerr (cubic) nonlinearity, $\delta n = n_2|u|^2$ (with $n_2>0$). Solitons in the one-dimensional (1D) version of Eq. (1), with the cubic nonlinear term and the sinusoidal transverse modulation, $n_0(x)=\epsilon\sin(2\pi x/\Lambda)$, were studied in Ref. [1]; later, the same equation, with u realized as the wave function of the Bose-Einstein condensate (BEC) and z replaced by time t, was considered in Ref. [2] [in that case, $n_0(x)$ represents an optical-lattice potential which traps the BEC]. Using numerical methods and a variational approximation (VA), it was shown that the model gives rise to a family of fundamental (single-peak) solitons, trapped in local waveguiding channels. The family of the fundamental solitons exists for all values $(0<Q<\infty)$ of the integral power, $Q\equiv\int_{-\infty}^{+\infty}|u(x)|^2dx$, which is a dynamical invariant of Eq. (1), and the entire family is stable. Symmetric double-peak solitons, which may be considered as bound states of in-phase fundamental beams,were also found in Ref. [1]. For fixed period Λ, the double-peak solitons exist above a certain minimum value, $k_{\min}$, of the propagation constant; attempts to create double-peak solitons with $k<k_{\min}$ result in the merger of the two peaks into a single one.

Non-Kerr nonlinearities give rise to new effects in the soliton dynamics, and, accordingly, suggest new possibilities for potential applications. The simplest nonlinearity in optical media deviating from the Kerr law combines the self-focusing cubic term and a self-defocusing quintic one (*competing nonlinearities*). The cubic-quintic (CQ) dielectric response was reported in chalcogenide glasses [3] and some organic optical materials [4] (it is necessary to mention that the CQ nonlinearity usually comes together with two-photon absorption [5]; however, it was shown in Ref. [6] that the nonlinear loss may be negligible for transmission distances which are sufficient to experiments with spatial solitons [7]).

The interplay of the CQ nonlinearity with the waveguide structure gives rise to *bistability* and *multistability* of soliton families. A bistable family of fundamental solitons trapped in a single guiding channel was reported in Ref. [8]. The bistability manifested itself in the appearance of two different branches of the family, provided that the channel's depth exceeded a threshold value. One branch, which continues the ordinary family of the soliton solutions, features the $Q(k)$ dependence with $dQ/dk>0$, hence it is expected to be stable, according to the Vakhitov-Kolokolov (VK) stability criterion [9]. The second branch exhibits a decreasing $Q(k)$ dependence, with $dQ/dk<0$; nevertheless, it was found to be stable too, *contrary* to the VK criterion (in fact, the validity of this criterion in models combining the CQ nonlinearity and transverse potential has not been proven).

A periodic structure most relevant to optical applications corresponds not to the above-mentioned sinusoidal effective potential, but rather to one in the form of a periodic array of rectangular channels, i.e., the effective potential of the Kronig-Penney (KP) type [10]. Families of 1D spatial solitons in the model combining the KP waveguiding structure

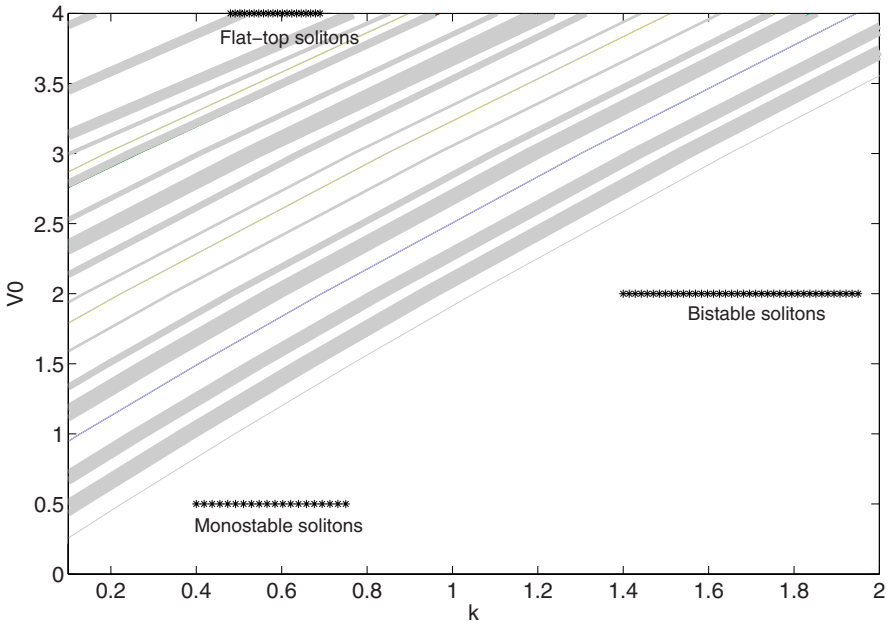

FIG. 1. (Color online) A typical example of the band-gap spectrum generated by the variation of depth V_0 of the 2D checkerboard potential with the fixed half-period, $D=3$ [see Eq. (3)] in the linearized version of Eq. (5). Bloch bands (where regular solitons cannot exist) are shaded. Marked segments represent various families of fundamental solitons found in the full nonlinear model, "flat-top" pertaining to the family of unstable gap solitons, see text.

with the CQ nonlinearity were studied in detail in Ref. [11] (1D solitons supported by the combination of the KP potential and cubic nonlinearity were considered in Ref. [12]). In addition to two coexisting stable branches of the fundamental solitons, similar to the above-mentioned ones which exist in the model with the single waveguiding channel [8], families of various higher-order solitons are supported by the KP potential. These include symmetric and antisymmetric double-peaked ones, two species of three-peaked patterns, with in-phase or out-of-phase central and side peaks, and others (in particular, five-peaked structures were found too). Similar to the fundamental solutions, each family of the multipeaked solitons features the bistability, i.e., two branches, with $dQ/dk>0$ and $dQ/dk<0$. All these solution families were found to be stable, irrespective of the formal compliance with the VK criterion (in Ref. [11], the stability was verified not only in direct simulations of the evolution of perturbed solitons, but also through computation of stability eigenvalues for small perturbations). The difference of the KP-CQ model from its single-channel counterpart, in which integral power Q of the fundamental soliton takes all values from 0 to ∞, while higher-order solitons do not exist [8], is that, in the presence of the periodic KP potential, the single-peak soliton exists up to a maximum value, $Q_{\max}^{(\mathrm{single})}$, above which only multihumped solitons are found. Continuing this trend, the CQ-nonlinear KP model in one dimension features a *beam-splitting* property: solitons with any number of peaks are stable, but they are found in a finite range of Q; further increase of the integral power results in consecutive appearance of additional peaks, i.e., subbeams trapped in adjacent channels of the KP structure, which leads to the change in the type of the pattern.

Another distinctive feature of the CQ model with the KP substrate is the band structure of the soliton solutions. Similar to the models combining the self-focusing Kerr nonlinearity and periodic potentials [1,2,12], the solitons are first of all found in the semi-infinite gap under the bottom of the Bloch-band structure induced by the periodic potential, while finite gaps between the Bloch bands remain empty (stable 1D solitons emerge in the finite band gaps too if the KP potential is strong enough, although these *gap solitons* do not feature bistability). However, in contrast to the model with the cubic nonlinearity, the band of fundamental-soliton solutions is itself *finite*, being located near the top of the semi-infinite gap, while its deeper part remains empty. Similar results for soliton families were also demonstrated in Ref. [13] in the model combining the CQ nonlinearity and the sinusoidal periodic potential (recently, an equivalent 1D model was derived in the context of BEC under the combined action of linear and nonlinear lattices [14]).

It is also relevant to mention that, if the periodic potential is very strong, it effectively splits the transversely continuous beam into strongly localized "beamlets," which are trapped in individual channels, and are linearly coupled by weak tunneling in the transverse direction. In this case, Eq. (1) may be approximately replaced by the discrete NLS equation. This approximation was elaborated in detail for the BEC trapped in a very deep optical lattice [15]. In the case of the CQ nonlinearity, the same approach leads to the CQ version of the discrete NLS equation, in which bright solitons were studied in detail in Ref. [16], and their dark counterparts in Ref. [17].

In the experiment, 2D spatial solitons supported by lattices have been created by shining beams with extraordinary polarization into a photorefractive medium (with saturable, rather than cubic or CQ nonlinearity), where *photonic lattices* were induced by a system of properly directed laser beams that illuminated the sample in the ordinary polarization (in which the medium is almost linear) [18], see also reviews [19]. In addition to the fundamental solitons, localized vortices [20], soliton necklaces [21], and solitons supported by radial photonic lattices [22] have been created by means of this technique. Also predicted were 2D photorefractive solitons that can be supported by the quasi-1D lattice (which corresponds to a potential periodic in x and indepen-

dent of y), the advantage of the latter setting being a possibility to simulate collisions between moving solitons [23].

Equation (1) in the 2D form, with the cubic self-focusing nonlinearity and sinusoidal potential, plays the role of the Gross-Pitaevskii equation for BEC in the "pancake"-shaped trap, supplemented with the 2D optical lattice. Stable fundamental and vortical solitons in that setting were found in Refs. [24,25]. In a similar model of photonic-crystal fibers (with both the refractive index and Kerr coefficient subjected to the periodic modulation corresponding to a lattice of voids running parallel to the propagation axis), spatial 2D solitons [26] and localized vortices [27] were predicted too. The latter model may also apply to a tightly packed bundle of silica fibers, which have recently been made available to the experiment [28].

The objective of the present work is to construct spatial solitons and localized vortices in the 2D *checkerboard* periodic potential (i.e., a 2D generalization of the KP lattice) with the CQ nonlinearity, the accordingly normalized equation (1) being

$$i\frac{\partial u}{\partial z} + \left(\frac{\partial^2}{\partial x^2} + \frac{\partial^2}{\partial y^2}\right)u + V_0 f_{\text{board}}(x,y)u + (2|u|^2 - |u|^4)u = 0, \tag{2}$$

where the "board" function is defined as a periodic array (with period $2D$) of waveguiding cores of width D, separated by buffer layers of the same width:

$$f_{\text{board}}(x,y) = \begin{cases} 1, & 2Dm < x < D(2m+1), \quad 2Dn < y < D(2n+1), \\ 1, & D(2m-1) < x < 2Dm, \quad D(2n-1) < y < 2Dn, \\ 0, & 2Dm < x < D(2m+1), \quad D(2n-1) < y < 2Dn, \\ 0, & D(2m-1) < x < 2Dm, \quad 2Dn < y < D(2n+1), \end{cases} \tag{3}$$

with $m,n=0,1,2,\ldots$. Once the form of Eq. (2) is fixed, parameters D and V_0 of the checkerboard potential are irreducible ones. Integral power

$$Q \equiv \int\int |u(x,y)|^2 dxdy \tag{4}$$

must be added to the set of D and V_0, as an intrinsic parameter of soliton families.

In this work, we aim to analyze, in particular, manifestations of the above-mentioned beam-splitting mechanism in the 2D setting, as well as the multistability of 2D spatial solitons and localized vortices. It is relevant to mention that the transmission of light beams through checkerboard structures built of ordinary and meta- (artificial) materials was considered (in the linear setting) in several works, see, e.g., Ref. [29]. The periodic structures were composed of various elements, such as rhombuses, triangles, etc. The 2D periodic potential of the KP type was also recently considered (but not in the context of competing nonlinearities) in Ref. [30].

The paper is organized as follows. In Sec. II, we report analytical results obtained by means of the variational approximation (VA) for fundamental solitons. The band-gap structure which is induced, in the linearized equation, by 2D checkerboard potential (3) is presented in the same section. Numerical results for the fundamental and multipeak (nontopological) solitons, and comparison with predictions of the VA, are reported in Sec. III. Stable vortex solitons of two types ("oblique" and "straight," either one based on a set of four local peaks) are presented in Sec. IV, where it is also shown that the most compact, "crater-shaped," vortices are unstable, transforming themselves into nontopological solitons which perform a persistent random walk on the checkerboard. The paper is concluded by Sec. V.

II. BAND-GAP SPECTRUM AND VARIATIONAL APPROXIMATION

Stationary soliton solutions to Eq. (2) are looked for in the usual form, $u(x,z)=\exp(ikz)R(x,y)$, where k is a real propagation constant, and function $R(x,y)$ (generally, a complex one) obeys the equation

$$\left(\frac{\partial^2}{\partial x^2} + \frac{\partial^2}{\partial y^2}\right)R + V_0 f_{\text{board}}(x,y)R + (2|R|^2 - |R|^4)R = kR. \tag{5}$$

Soliton solutions that can be found in this model should be identified in terms of the location of their propagation constant with respect to the band-gap spectrum of the linearized version of Eq. (5). A typical example of the spectrum, computed by means of approximating the respective linear operator by a large-size matrix, is displayed in Fig. 1.

For fundamental solitons, function $R(x,y)$ is real. In that case, aiming to develop the VA in an analytically tractable form, we decompose the "board potential," defined by Eq. (3), into the 2D Fourier series, in which only the two lowest harmonics are kept (the latter approximation is obviously relevant when the size of the soliton is much larger than the lattice period $2D$; for more narrow solitons, it may still be adopted as a reasonable simplification). Further, it is convenient to rotate the coordinate axes by 45° and define

$$\{\xi,\eta\} \equiv \frac{(x \pm y)}{\sqrt{2}}, \quad K \equiv k - \frac{V_0}{2}, \quad q \equiv \frac{\sqrt{2}\pi}{D}, \quad \varepsilon = \left(\frac{4}{\pi^2}\right)V_0. \tag{6}$$

Then, Eq. (5) (for real R) with the simplified periodic potential takes the form of

$$\left(\frac{\partial^2}{\partial\xi^2} + \frac{\partial^2}{\partial\eta^2}\right)R + \varepsilon[\cos(q\xi) + \cos(q\eta)]R + 2R^3 - R^5 = KR. \tag{7}$$

Equation (7) can be derived from the Lagrangian, $L = \int\int \mathcal{L} d\xi d\eta$, with density

$$2\mathcal{L} = \left[\left(\frac{\partial R}{\partial \xi}\right)^2 + \left(\frac{\partial R}{\partial \eta}\right)^2\right] + KR^2 - \varepsilon[\cos(q\eta) + \cos(q\eta)]R^2 - R^4 + \frac{1}{3}R^6. \tag{8}$$

The ansatz for the fundamental soliton is adopted in the ordinary Gaussian form [24],

$$R(\xi,\eta) = A\exp[-(a/2)(\xi^2 + \eta^2)] \tag{9}$$

(with $a > 0$). The substitution of the ansatz in Lagrangian density (8) and integration yield the *effective Lagrangian*,

$$2L_{\text{eff}} = KQ + aQ - 2\varepsilon Q\exp\left(-\frac{q^2}{4a}\right) - \frac{aQ^2}{2\pi} + \frac{a^2Q^3}{9\pi^2}, \tag{10}$$

where the total power, defined by Eq. (4) is $Q = \pi A^2/a$ for ansatz (9).

Lagrangian (10) gives rise to two variational equations, $\partial L_{\text{eff}}/\partial Q = 0$, and $\partial L_{\text{eff}}/\partial a = 0$, i.e.,

$$K + a - 2\varepsilon\exp\left(-\frac{q^2}{4a}\right) - \frac{aQ}{\pi} + \frac{a^2Q^2}{3\pi^2} = 0,$$

$$1 - \frac{Q}{2\pi} + \frac{2aQ^2}{9\pi^2} - \frac{\varepsilon q^2}{2a^2}\exp\left(-\frac{q^2}{4a}\right) = 0. \tag{11}$$

Straightforward analysis of Eqs. (11) demonstrates that the limit of $Q \to \infty$ corresponds to $a \approx 9\pi/(4Q)$ and $K \to K_\infty = 9/16$. Analytical expressions can also be derived from these equations for coordinates of the *turning point* (TP) in dependence $Q(K)$, for those cases when the VA predicts the bistability, see Fig. 5 below:

$$K_{\text{TP}} = \frac{45}{64} - \frac{9\pi}{8}\left(1 + \frac{9}{8q^2}\right)\frac{1}{Q_{\text{TP}}} + \frac{81\pi^2}{16q^2}\frac{1}{Q_{\text{TP}}^2},$$

$$a_{\text{TP}} = \frac{9\pi}{8Q_{\text{TP}}}, \tag{12}$$

the respective value of the lattice's depth being

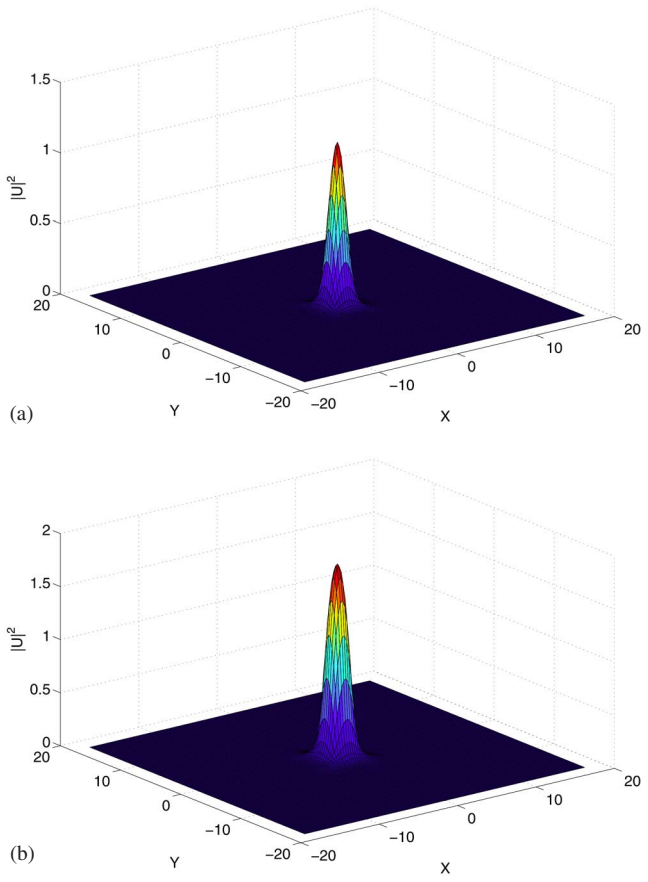

FIG. 2. (Color online) "Low" (a) and "tall" (b) stable fundamental solitons with equal wave numbers, $k = 1.8$ (it falls in the semi-infinite gap, whose border is located at $k = 1.04$, in the present case), and powers $Q_a = 5.46$ and $Q_b = 11.52$, respectively. The half-period of the Kronig-Penney potential structure is $D = 3$ (all plots displayed below also pertain to $D = 3$), and its depth is $V_0 = 2$ (other plots are shown for the same value of V_0, unless specified otherwise).

$$\varepsilon_{\text{TP}} = \frac{a_{\text{TP}}}{q^2}\left(2a_{\text{TP}} - \frac{9}{16}\right)\exp\left(\frac{q^2}{4a_{\text{TP}}}\right). \tag{13}$$

The predictions of the VA will be displayed and compared to numerical findings in the next section.

III. FUNDAMENTAL AND HIGHER-ORDER SOLITONS

Numerical solutions to Eq. (5) were constructed by means of the relaxation method. They reveal many species of localized states with k falling in the semi-infinite band gap (see Fig. 1). Unless the lattice is too shallow (V_0 too small), all solution families feature the bistability, with two different solutions ("tall" and "low" ones) found at a given value of k. The simplest type of the solutions represents fundamental (single-peak) solitons. An example of a pair of bistable fundamental solitons, whose integral powers differs by a factor of ≈ 2, is displayed in Fig. 2.

With the increase of integral power Q, the beam-splitting property in the 2D setting manifests itself differently from the 1D model [11]: when the power of the fundamental beam attains the largest value up to which the fundamental soliton

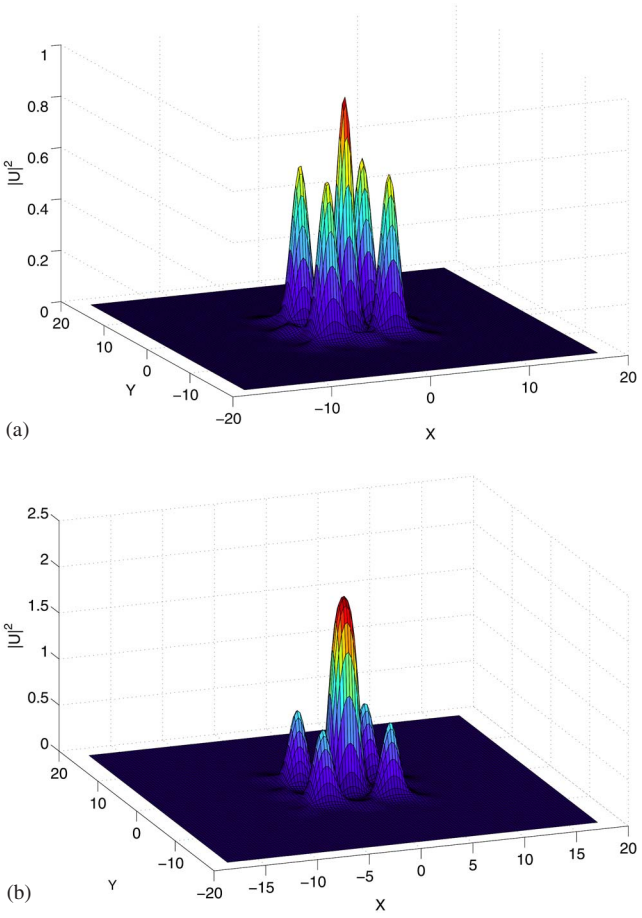

FIG. 3. (Color online) Stable "low" (a) and "tall" (b) five-peak solitons with the same wave number, $k=1.5$, which belongs to the semi-infinite gap; the respective powers are $Q_a=15.6$ and $Q_b=28.12$.

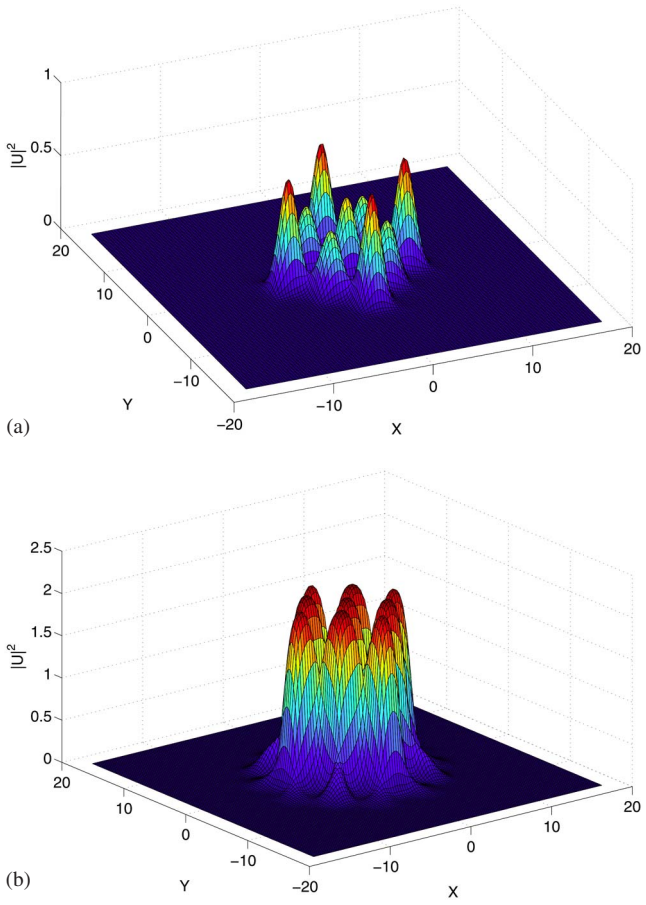

FIG. 4. (Color online) Stable "low" (a) and "tall" (b) nine-peak solitons with equal wave numbers, $k=1.7$, and powers $Q_a=28.51$ and $Q_b=199.39$.

may exist, the competition of the cubic and quintic nonlinearities forces the beam to create extra "humps" not on two sides of the central peak (as it did in the 1D model), but on its four sides, along the two diagonals passing through the center. Thus the next family of 2D localized solutions, after the single-peak solitons, includes five-peak patterns, and this family also features the bistability, as shown in Fig. 3.

Following the same scenario, nine-peak bistable localized patterns naturally emerge in the 2D KP setting with the subsequent increase of Q, see an example in Fig. 4. More complex bistable structures were found too, at still larger values of Q.

The entire family of the fundamental solitons is shown in Fig. 5(a) by means of curves $Q(k)$, for three characteristic values of the lattice depth, which correspond to the monostable family, emerging bistability, and well-pronounced bistability, respectively. For all three cases, both the numerically found curves and their counterparts, predicted by the VA via Eqs. (11) and (6), are displayed in Fig. 5(a). Additionally, Fig. 5(b) presents the VA-numerical comparison for the turning point in the $Q(k)$ dependence [provided that this point exists, i.e., the $Q(k)$ curve features the bistability]. The latter plot collects numerical data not only for the fundamental solitons, but also for their higher-order counterparts, as the VA tends to approximate them all by ansatz (9). It is seen that the VA provides good accuracy only in shallow lattices; nevertheless, the VA is able to predict the transition from the monostability to bistability with the increase of the lattice's depth. Note that the locus of the turning points is predicted by the VA better than particular $Q(k)$ characteristics in the deep lattice.

Intervals in which mono- and bistable families of the fundamental solitons were found, at $V_0=0.5$ and 2, respectively, in the semi-infinite gap, are also shown in Fig. 1. The ends of the intervals are those points beyond which the soliton families cannot be extended, cf. Fig. 5(a).

Similar numerically found characteristics for the families of the five- and nine-peak solutions are shown in Fig. 6; for the sake of the comparison, the family of the fundamental solitons (the one found in the numerical form) in included in this figure too, at the same value of the lattice depth, $V_0=2$. The picture gives a clear idea of the multistability of various types of solitons in the 2D CQ model with a sufficiently deep periodic potential. As well as in Fig. 5(a), all the solution families displayed in this figure terminate at end points (no solution could be found beyond those points). It is worthy to note that, while the five-peak solitons emerge at the maximum value of Q at which the fundamental beams cease to exist, in precise compliance with the beam-splitting prin-

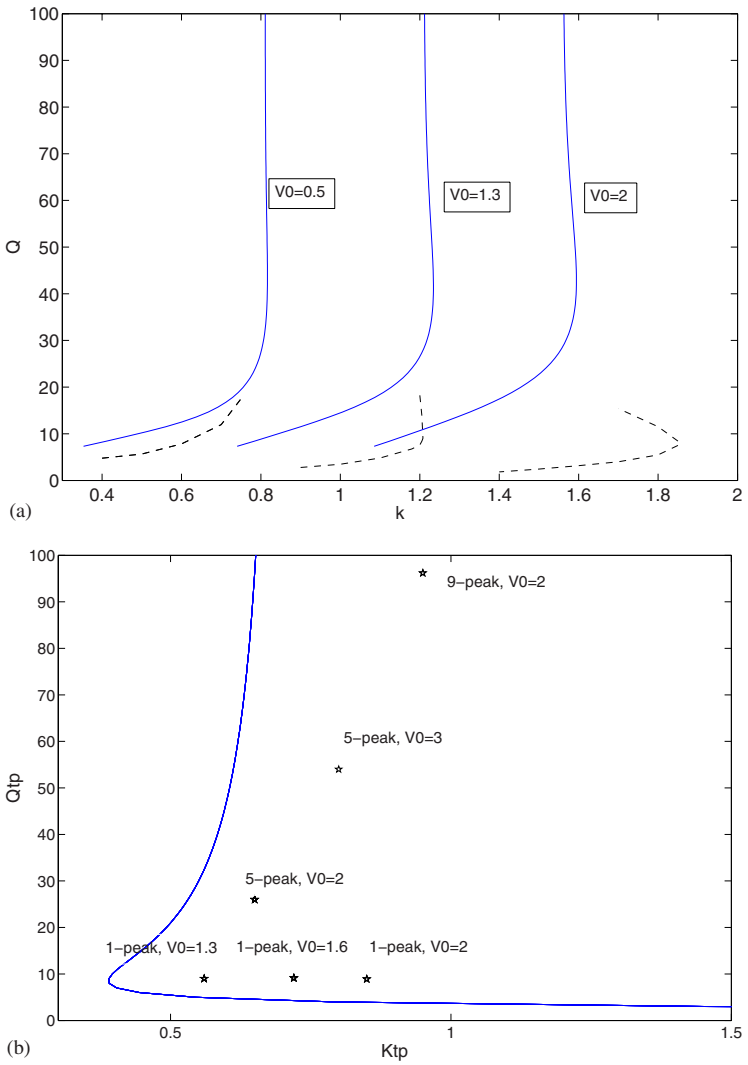

FIG. 5. (Color online) (a) Characteristics $Q(k)$ (integral power versus the wave number), as predicted by the variational approximation and found from the numerical solution (solid and dashed lines, respectively), for typical cases of shallow, intermediate-depth, and relatively deep Kronig-Penney lattice potential. All the curves representing the numerical results terminate at points beyond which fundamental solitons could not be found. (b) Comparison between the locus of the turning points in the $Q(k)$ dependence, predicted by the variational approximation (solid curves) and their counterparts (stars), numerically found for both the fundamental and higher-order solitons (the values of V_0 and the type of the corresponding solution are indicated in the panel).

ciple, the family of the nine-peak solitons partly overlaps, in terms of Q, with the range of five-peak solitons, which gives rise to the bistability of a different kind, viz., the coexistence of stable solitons with different numbers of peaks at common values of the total power (of course, they correspond to different values of k).

Figures 1, 5, and 6 also clearly show another feature of the CQ model, which is stipulated by the competition of the self-focusing and self-defocusing nonlinearities: the solution families occupy only finite regions in the semi-infinite gap. A similar feature was reported in the 1D version of the model [11].

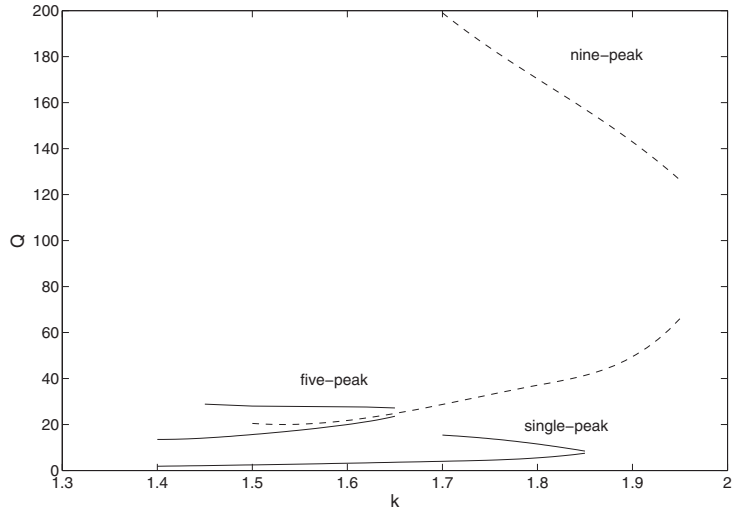

FIG. 6. Numerically obtained power-versus-wave-number characteristics for the families of fundamental and higher-order solitons in the region of bistability of each family. The curves representing the nine-peak family are disconnected because of difficulties with finding the respective sophisticated solutions, close to the turning point, by means of the relaxation method.

Direct numerical simulations of the evolution of initially perturbed solitons clearly demonstrate that all the soliton families found in the semi-infinite band gap, both fundamental and higher-order ones, are completely stable (the stability simulations are not displayed here as they do not convey noteworthy features). As mentioned above in the context of the 1D counterpart of the present model [8,11], both branches of the solution families which feature the turning point are stable, despite the fact that only one branch satisfies the VK criterion, $dQ/dk>0$ (i.e., this criterion is not relevant to the CQ model with a waveguiding potential). In the case when the stable five- and nine-peak solitons coexist, see Fig. 6, the established pattern depends on the initial condition: the input in the form of a very broad uniform beam tends to split into nine peaks, while a more compact beam gives rise to five peaks.

For sufficiently large values of V_0 (deep lattice), solitons were also found in finite gaps of the band-gap spectrum. Unlike the fundamental solitons in the semi-infinite band gap, the finite-gap solitons feature a flat shape in the central part, and conspicuous tails attached to it along the diagonal directions, see an example in Fig. 7(a). However, all such solitons whose stability was tested were found to be *unstable*, see a typical example in Fig. 7(b). This instability is a drastic difference from finite-gap solitons found in the deep KP lattice in the 1D model, where they are mostly stable [11].

The $Q(k)$ characteristics for families of the 2D solitons in finite band gaps feature no bistability. Those characteristics are not shown here, but the interval in which the gap solitons were found in the model at $V_0=4$ is labeled in Fig. 1 as "flat-top solitons." Even though these solitons are unstable, it is worthy to note that their family is found not only in the finite band gap, but also extends into the adjacent Bloch band, inside of which the solitons change their character from regular to becoming *embedded solitons* [31].

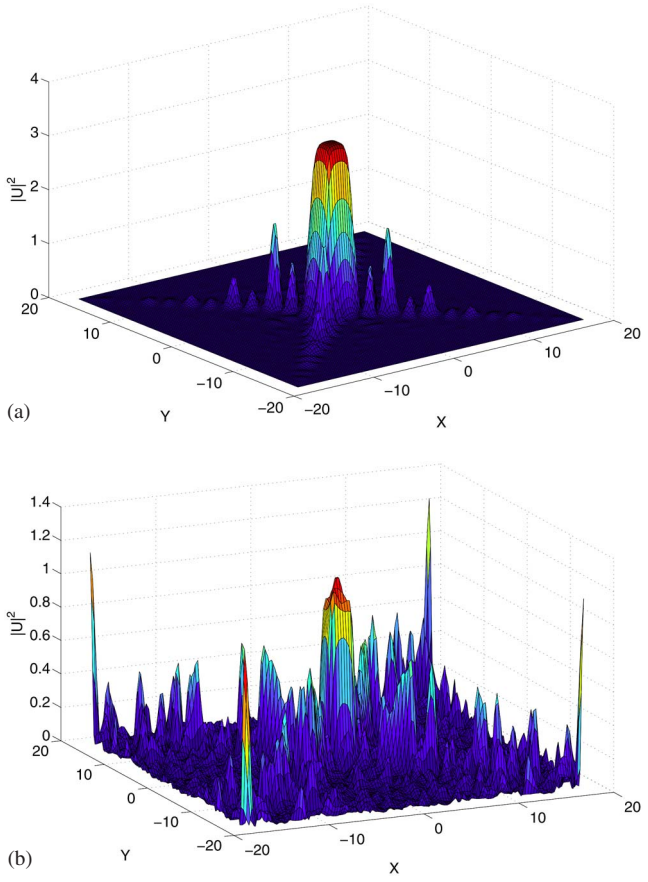

FIG. 7. (Color online) (a) An example of a soliton found inside a finite band gap (for $k=0.6$, the soliton's integral power being $Q=70.9$) in a deep lattice, with $V_0=4$. (b) A result of the development of the instability of this soliton, after passing distance $z=35$ (which is tantamount to $\simeq 9$ diffraction lengths of the unperturbed soliton). The initial random perturbation was imposed with relative amplitude 5%.

IV. VORTEX SOLITONS

The 2D model opens the way to find topological solitons with intrinsic vorticity, which are represented by complex localized solutions to Eq. (3) with the phase circulation of $2\pi S$ around the central point, $r=0$ (at which the local amplitude vanishes as r^S), the positive integer S being the topological charge (vorticity). In the 2D model with the cubic self-focusing nonlinearity and sinusoidal periodic potential, examples of stable localized vortices with $S=1$ were reported in Refs. [24,25]. Stable higher-order vortices (up to $S=6$), as well as multipoles (structured multipeak solitons with zero net topological charge) and "supervortices" (ringlike chains of compact vortices, each with individual charge s, and independent global vorticity S imprinted onto the chain), were found in Ref. [32].

Here, we focus on the search for vortex-beam solutions belonging to the semi-infinite gap [vortices were also found in finite band gaps, but they all appear to be unstable there, as well as their fundamental-soliton counterparts, see Fig. 7(b)]. First, we have found compact ("crater-shaped") vortex solitons, which are trapped, essentially, in a single cell of the KP potential, see Fig. 8(a). However, all vortices of this type turn out to be unstable (the same conclusion was made in the model combining the cubic nonlinearity and the sinusoidal potential [24]; nevertheless, stable supervortices reported in Ref. [32] were constructed as chains of crater-shaped individual vortices, with $s=\pm 1$, i.e., such individually unstable objects may build stable complexes, due to their mutual interactions). The instability splits the crater-shaped vortex into a set of nonsteady fundamental beams, with a single one surviving in the course of the evolution, as shown in Fig. 8(b). This remaining fundamental (quasi-)soliton performs random motion across the lattice (keeping its integrity), see Fig. 8(c), until hitting a border of the integration domain. This picture also demonstrates the possibility of the motion of fundamental solitons across the (shallow) KP lattice in two dimensions.

Two species of stable vortex solitons with $S=1$ have been found in the present model. Either one features a set of four local peaks, with the phase shift of $\pi/2$ between them, which corresponds to topological charge $S=1$. The first species, which may be called "oblique," as opposite peaks in the pattern are connected by diagonals of the KP lattice, is dis-

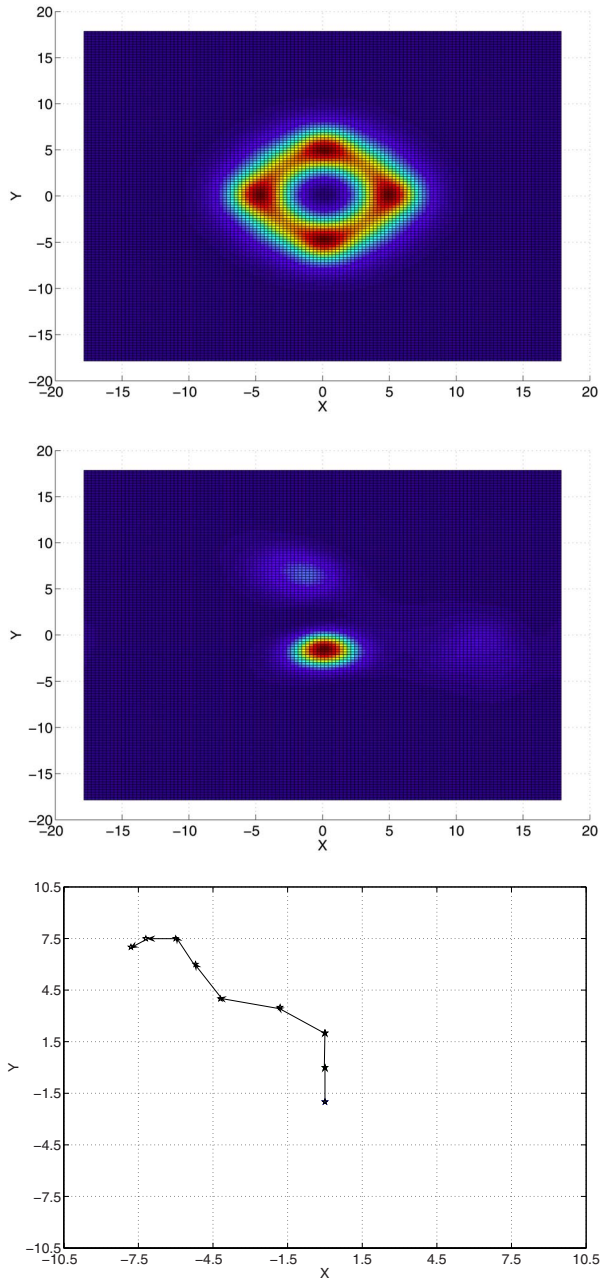

FIG. 8. (Color online) (a) An unstable compact ("crater-shaped") vortex, with $S=1$, $k=0.2$, and total power $Q=27.68$, is shown by means of the local-power contour plots, $|u(x,y)|^2$, in the shallow lattice, with $V_0=0.1$. (b) The result of the instability development of the compact vortex: spontaneous transformation into a single-peak quasisoliton, with power $Q=11.53$, at $z=40$. (c) The trajectory of the random walk of the quasisoliton displayed in panel (b). The total propagation distance corresponding to panel (c) amounts to ~ 10 diffraction lengths of the walking beam. In this and the next figure, the grid represents the 2D Kronig-Penney lattice potential, with half-period D equal to the spacing between lines forming the grid.

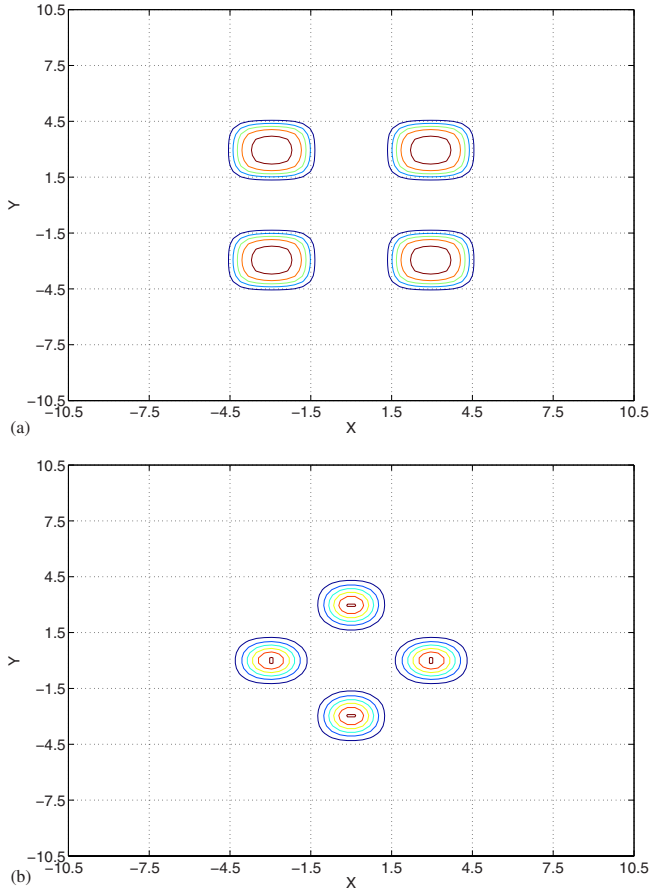

FIG. 9. (Color online) Examples of two types of stable vortex solitons (with $S=1$) in the strong KP lattice ($V_0=10$) are shown by means of contour plots: (a) an *oblique vortex* (the one with an almost empty site at the center), which has $k=8$ and $Q=69.79$ and (b) a more compact *straight vortex*, with $k=9$ and $Q=7.29$.

played in Fig. 9(a). It resembles stable vortices reported in Refs. [24,25], in the above-mentioned model based on the 2D cubic-NLS equation with the sinusoidal lattice potential. The other species, "straight vortex" (so-called because the opposite peaks are connected by lines running parallel to the lattice bonds), is shown in Fig. 9(b). In previously considered 2D models combining the cubic nonlinearity and lattice potentials, this type of stable vortices was not reported, as far as we know; however, both species of vortex solitons are known in discrete 2D models, where they are sometimes called "crosses" and "squares," respectively [33]. The crucial distinction between the species is that the oblique vortices are less densely packed, including a nearly empty lattice site at the center, while the straight vortex sets its center between the sites, thus not leaving any internal lattice cell vacant.

Direct simulations (not shown here) confirm that both vortex-soliton species, the oblique and straight ones, are very robust to perturbations, and families of these vortices also feature the bistability. In addition to them, higher-order vortices, with $S \geq 2$, above-mentioned "supervortices," and other types of stable structured multipeak patterns, such as dipoles and quadrupoles, can be found in the present model. They will be reported in a systematic form elsewhere.

V. CONCLUSIONS

We have introduced the 2D version of the model combining the periodic KP (Kronig-Penney) potential, alias the

checkerboard, and the competing CQ (cubic-quintic) nonlinearity. The main objectives of the analysis were to examine the beam-splitting mechanism and soliton multistability in this setting, as suggested by the recently studied 1D version of the KP-CQ model. Families of fundamental and multipeak higher-order solitons have been found in the semi-infinite gap, where each family features the bistability, unless the KP lattice is too shallow. In direct simulations, both branches of each bistable family are stable against arbitrary perturbations, disobeying the VK (Vakhitov-Kolokolov) criterion. For fundamental solitons, the VA (variational approximation) was developed too, which provides a qualitatively correct description of the soliton families, including the transition from monostability to the bistability. Solitons in finite band gaps were also found, but they appear to be unstable. Vortex solitons, structured as four-peak sets with appropriate phase shifts, were constructed too. They feature two different types, oblique and straight ones, both being stable in the semi-infinite gap (the latter one was not considered before in continuous models, although its counterpart is known as a "square vortex" in discrete lattices). On the contrary to that, the compact "crater-shaped" vortices are unstable. They spontaneously transform themselves into nonsteady (but robust) fundamental beams, which perform a random walk in the lattice, provided that it is shallow enough.

The solitons and vortices predicted in this work can be created in optical media which feature the CQ nonlinearity, such as chalcogenide glasses and some organic materials. These solitary beams may find applications to the design of multichannel all-optical data-processing systems.

ACKNOWLEDGMENTS

We appreciate a discussion with B. B. Baizakov. The work of R.D. was supported by the Chateaubriand Foundation.

[1] B. A. Malomed, Z. H. Wang, P. L. Chu, and G. D. Peng, J. Opt. Soc. Am. B **16**, 1197 (1999).
[2] G. L. Alfimov, V. V. Konotop, and M. Salerno, Europhys. Lett. **58**, 7 (2002); V. A. Brazhnyi and V. V. Konotop, Mod. Phys. Lett. B **18**, 627 (2004).
[3] F. Smektala, C. Quemard, V. Couderc, and A. Barthélémy, J. Non-Cryst. Solids **274**, 232 (2000); K. Ogusu, J. Yamasaki, S. Maeda, M. Kitao, and M. Minakata, Opt. Lett. **29**, 265 (2004).
[4] C. Zhan, D. Zhang, D. Zhu, D. Wang, Y. Li, D. Li, Z. Lu, L. Zhao, and Y. Nie, J. Opt. Soc. Am. B **19**, 369 (2002).
[5] G. Boudebs, S. Cherukulappurath, H. Leblond, J. Troles, F. Smektala, and F. Sanchez, Opt. Commun. **219**, 427 (2003); F. Sanchez, G. Boudebs, S. Cherukulappurath, H. Leblond, J. Troles, and F. Smektala, J. Nonlinear Opt. Phys. Mater. **13**, 7 (2004).
[6] Y.-F. Chen, K. Beckwitt, F. W. Wise, and B. A. Malomed, Phys. Rev. E **70**, 046610 (2004).
[7] S. Maneuf and F. Reynaud, Opt. Commun. **65**, 325 (1988); J. S. Aitchison, A. M. Weiner, Y. Silberberg, M. K. Oliver, J. L. Jackel, D. E. Leaird, E. M. Vogel, and P. W. E. Smith, Opt. Lett. **15**, 471 (1990).
[8] B. V. Gisin, R. Driben, and B. A. Malomed, J. Opt. B: Quantum Semiclassical Opt. **6**, S259 (2004).
[9] N. G. Vakhitov and A. A. Kolokolov, Izv. Vyssh. Uchebn. Zaved., Radiofiz. **16**, 10120 (1973) [Radiophys. Quantum Electron. **16**, 783 (1973)].
[10] R. de L. Kronig and W. G. Penney, Proc. R. Soc. London, Ser. A **130**, 499 (1931); C. Kittel, *Introduction to Solid State Physics* (Wiley, New York, 1995).
[11] I. M. Merhasin, B. V. Gisin, R. Driben, and B. A. Malomed, Phys. Rev. E **71**, 016613 (2005).
[12] W. D. Li and A. Smerzi, Phys. Rev. E **70**, 016605 (2004).
[13] J. Wang, F. Ye, L. Dong, T. Cai, and Y.-P. Li, Phys. Lett. A **339**, 74 (2005).
[14] F. Abdullaev, A. Abdumalikov, and R. Galimzyanov, Phys. Lett. A **367**, 149 (2007).
[15] A. Trombettoni and A. Smerzi, Phys. Rev. Lett. **86**, 2353 (2001); G. L. Alfimov, P. G. Kevrekidis, V. V. Konotop, and M. Salerno, Phys. Rev. E **66**, 046608 (2002); N. K. Efremidis and D. N. Christodoulides, Phys. Rev. A **67**, 063608 (2003); A. Smerzi and A. Trombettoni, Chaos **13**, 766 (2003).
[16] R. Carretero-González, J. D. Talley, C. Chong, and B. A. Malomed, Physica D **216**, 77 (2006).
[17] A. Maluckov, L. Hadžievski, and B. A. Malomed, Phys. Rev. E **76**, 046605 (2007).
[18] J. W. Fleischer, M. Segev, N. K. Efremidis, and D. N. Christodoulides, Nature (London) **422**, 147 (2003).
[19] J. W. Fleischer, G. Bartal, O. Cohen, T. Schwartz, O. Manela, B. Freedman, M. Segev, H. Buljan, and N. K. Efremidis, Opt. Express **13**, 1780 (2005); A. S. Desyatnikov, N. Sagemerten, R. Fischer, B. Terhalle, D. Träger, D. N. Neshev, A. Dreischuh, C. Denz, W. Krolikowski, and Y. S. Kivshar, *ibid.* **14**, 2851 (2006).
[20] D. N. Neshev, T. J. Alexander, E. A. Ostrovskaya, Y. S. Kivshar, H. Martin, I. Makasyuk, and Z. G. Chen, Phys. Rev. Lett. **92**, 123903 (2004); J. W. Fleischer, G. Bartal, O. Cohen, O. Manela, M. Segev, J. Hudock, and D. N. Christodoulides, *ibid.* **92**, 123904 (2004).
[21] J. Yang, I. Makasyuk, P. G. Kevrekidis, H. Martin, B. A. Malomed, D. J. Frantzeskakis, and Z. Chen, Phys. Rev. Lett. **94**, 113902 (2005).
[22] X. Wang, Z. Chen, and P. G. Kevrekidis, Phys. Rev. Lett. **96**, 083904 (2006).
[23] T. Mayteevarunyoo and B. A. Malomed, Phys. Rev. E **73**, 036615 (2006).
[24] B. B. Baizakov, B. A. Malomed, and M. Salerno, Europhys. Lett. **63**, 642 (2003).
[25] J. Yang and Z. H. Musslimani, Opt. Lett. **28**, 2094 (2003); Z. H. Musslimani and J. Yang, J. Opt. Soc. Am. B **21**, 973 (2004).
[26] P. Xie, Z.-Q. Zhang, and X. Zhang, Phys. Rev. E **67**, 026607 (2003); A. Ferrando, M. Zacares, P. F. de Cordoba, D. Binosi, and J. A. Monsoriu, Opt. Express **11**, 452 (2003).
[27] A. Ferrando, M. Zacares, P. F. de Cordoba, D. Binosi, and J. A.

Monsoriu, Opt. Express **12**, 817 (2004).
[28] A. Szameit, D. Blömer, J. Burghoff, T. Schreiber, T. Pertsch, S. Nolte, A. Tünnermann, and F. Lederer, Opt. Express **13**, 10552 (2005).
[29] X.-H. Wang, B.-Y. Gu, Z.-Y. Li, and G.-Z. Yang, Phys. Rev. B **60**, 11417 (1999); M. Agio and L. C. Andreani, *ibid.* **61**, 15519 (2000); S. A. Ramakrishna, S. Guenneau, S. Enoch, G. Tayeb, and B. Gralak, Phys. Rev. A **75**, 063830 (2007).
[30] Y. Sivan, G. Fibich, N. K. Efremidis, and S. Bar-Ad, e-print arXiv:0707.1589.
[31] J. Yang, B. A. Malomed, and D. J. Kaup, Phys. Rev. Lett. **83**, 1958 (1999); A. R. Champneys, B. A. Malomed, J. Yang, and D. J. Kaup, Physica D **152-153**, 340 (2001).
[32] H. Sakaguchi and B. A. Malomed, Europhys. Lett. **72**, 698 (2005).
[33] P. G. Kevrekidis, D. J. Frantzeskakis, R. Carretero-Gonzalez, B. A. Malomed, and A. R. Bishop, Phys. Rev. E **72**, 046613 (2005).